Activation cross section measurement of the deuteron-induced reaction on yttrium-89 for zirconium-89 production

Michiya Sakaguchi[1,*], Masayuki Aikawa[1,2], Moemi Saito[1], Naoyuki Ukon[3], Yukiko Komori[4] and Hiromitsu Haba[4]

[1] *Graduate School of Biomedical Science and Engineering, Hokkaido University, Sapporo 060-8638, Japan*

[2] *Faculty of Science, Hokkaido University, Sapporo 060-0810, Japan*

[3] *Advanced Clinical Research Center, Fukushima Medical University, Fukushima 960-1295, Japan*

[4] *Nishina Center for Accelerator-Based Science, RIKEN, Wako 351-0198, Japan*

Abstract

Activation cross sections of the deuteron-induced reactions on ^{89}Y were measured up to 24 MeV deuteron energy. The experiment was performed at the RIKEN AVF cyclotron. Excitation functions of the reactions ^{89}Y(d,x)^{88,89}Zr, ^{88,90m}Y, ^{87m}Sr were obtained by using the stacked-foil activation method and gamma-ray spectrometry. The results were compared with previous experimental data and the prediction of the TALYS nuclear reaction model code adopted from TENDL-2017 library. Physical thick target yield of ^{89}Zr was derived from the measured cross sections.

Keyword

Zirconium-89, PET technology, Deuteron-induced reaction

1. Introduction

Zirconium-89 ($T_{1/2} = 78.41$ h) is a positron emitter suitable for imaging via Positron Emission Tomography (PET). It has much longer half-life than fluorine-18 ($T_{1/2} = 109.77$ min), which is most widespread radionuclide in the field of PET radiopharmaceuticals. ^{89}Zr is particularly suitable for imaging biological processes with slow kinetics, e.g. in immuno-PET [1]. Its long half-life allows for transporting on large distances. A cost-effective delivery of ^{89}Zr requires detailed knowledge of its potential production routes.

High-specific activity ^{89}Zr can be produced in several charged-particle-induced nuclear reactions on various stable nuclides. Among them, reactions on ^{89}Y are the most favorable regarding the yield and possibility to bombard naturally monoisotopic element (low price of the target material, minimizing number of the co-produced radionuclides).

The ^{89}Y(p,n)^{89}Zr and the ^{89}Y(d,2n)^{89}Zr reactions are the most promising. There were many experiments performed on the former reaction during the last several decades (see e.g. [2] and references therein). In contrast, only eight experiments focused on the latter can be found in the literature survey [3–10]. The published excitation functions are not always entirely consistent and only a few previous studies measured data beyond 20 MeV. These facts lead us to re-measurement of the deuteron-induced reaction cross-sections on ^{89}Y up to 24 MeV.

* Corresponding author: michiya@nds.sci.hokudai.ac.jp

2. Method

For the measurement, we adopted a well-known and established stacked-foil activation technique. The target was composed of thin metallic foils of ^{89}Y (purity: 99.0%, thickness: 12.68 mg/cm^2; Goodfellow Co., Ltd., UK) and ^{nat}Ti (purity: 99.6%, thickness: 9.13 mg/cm^2; Nilaco Corp., Japan). The average thicknesses of the foils were derived from their weight and area before processing. The foils were then cut into squares of 8 × 8 mm^2 area. Nine sets of four Y and two Ti foils were stacked as the target. The foils other than the first one in the same element groups were measured because of expected compensation for recoil losses of the products. The ^{nat}Ti foils were used for reproduction of the ^{nat}Ti(d,x)^{48}V monitor reaction to adjust thicknesses of the foils and to check the beam parameters. This stacked target was positioned in a target holder that served as a Faraday cup and irradiated by a deuteron beam for 1 h at the RIKEN AVF cyclotron. The average beam intensity measured by the Faraday cup was 102.3 nA. The incident beam energy of 23.6 ± 0.2 MeV was measured by the time-of-flight method [11]. The energy loss of the projectile in each foil and its propagated uncertainty were calculated using the SRIM code [12].

The irradiated foils were disassembled after a cooling time of approximately 1 h. The gamma-ray spectra of each foil were measured by using an HPGe detector (ORTEC GEM30P4-70) without chemical separation. Calibration of the detector efficiency at each distance was performed by using the standard ^{152}Eu source and the mixed gamma-ray standard composed of ^{57,60}Co, ^{85}Sr, ^{88}Y, ^{109}Cd, ^{133}Sn, ^{137}Cs, ^{139}Ce, ^{203}Hg and ^{241}Am. The distance between the measured foils and the HPGe detector was adjusted to keep the dead time less than 5%.

Table 1 summarizes deuteron-induced reactions resulting in radionuclides for beam energies below 23.6-MeV. The radionuclides and their nuclear data are shown in Table 2. We measured gamma-ray spectra several times in order to optimize quantification of the present radionuclides with different half-lives.

The cross section σ (cm^2) can be derived from the equation:

$$\sigma = \frac{\lambda N}{n_T I \varepsilon_d \varepsilon_\gamma \varepsilon_t (1 - e^{-\lambda T_b}) e^{-\lambda T_c} (1 - e^{-\lambda T_m})}$$

where λ is the decay constant of a radionuclide (s^{-1}), N are the net counts in the gamma-line, n_T is the surface density of target atoms (cm^{-2}), I is the deuteron-beam intensity (s^{-1}), ε_d is the detector efficiency, ε_γ is the gamma-line intensity, ε_t is the dead time correction, T_b is the irradiation time of the beam (s), T_c is the cooling time (s) and T_m is the measurement time (s).

The cross sections of the ^{nat}Ti(d,x)^{48}V monitor reaction were derived to assess the target thicknesses and the beam parameters. Figure 1 shows the excitation function for this reaction together with the IAEA recommended values [15].

The thicknesses of the ^{89}Y foils were corrected by +2% within uncertainty to fit the recommended values. On the other hand, the measured beam parameters were adopted without any corrections since amplitudes of the derived cross sections originally showed a good agreement with the recommended values. The corrected thicknesses of the ^{89}Y foils are 12.93 mg/cm^2. We adopted them for the analysis in the next section.

Table 1. Possible reactions in this experiment with their Q-values and thresholds [13].

Reaction	Q-value (MeV)	Threshold energy (MeV)
^{89}Y(d,2n)^{89}Zr	-5.8	6.0
^{89}Y(d,3n)^{88}Zr	-15.2	15.5
^{89}Y(d,p)^{90m}Y	4.6	0
^{89}Y(d,p2n)^{88}Y	-13.7	14.0
^{89}Y(d,dn)^{88}Y	-11.5	11.7
^{89}Y(d,t)^{88}Y	-5.2	5.3
^{89}Y(d,tn)^{87m,g}Y	-14.6	14.9
^{89}Y(d,α)^{87m}Sr	7.9	0
^{89}Y(d,2d)^{87m}Sr	-16.0	16.3
^{89}Y(d,dpn)^{87m}Sr	-18.2	18.6
^{89}Y(d,tp)^{87m}Sr	-11.9	12.2
^{89}Y(d,n^{3}He)^{87m}Sr	-12.7	13.0
^{89}Y(d,α2n)^{85m,g}Sr	-12.0	12.3

The Q-values and threshold energies refer to formation of the ground states.

Table 2. Produced radionuclides and their nuclear data [14].

Radionuclide	Decay mode	Half-life	E_γ (keV)	I_γ (%)
^{89g}Zr	β^++EC : 100%	78.41 h	909.15	99.04
^{88}Zr	EC : 100%	83.4 d	392.87	97.29
^{90m}Y	IT : 100%	3.19 h	202.53	97.3
^{88}Y	β^++EC : 100%	106.627 d	898.042	93.7
^{87m}Y	IT : 98.43%	13.37 h	380.79	78.05
	β^++EC : 1.57%			
^{87}Y	β^++EC : 100%	79.8 h	484.805	89.8
^{87m}Sr	IT : 99.7%	2.815 h	388.531	82.19
	EC : 0.3%			
^{85m}Sr	IT : 86.6%	67.63 m	231.860	83.9
	EC : 13.4%			
^{85g}Sr	EC : 100%	64.849 d	514.0048	96

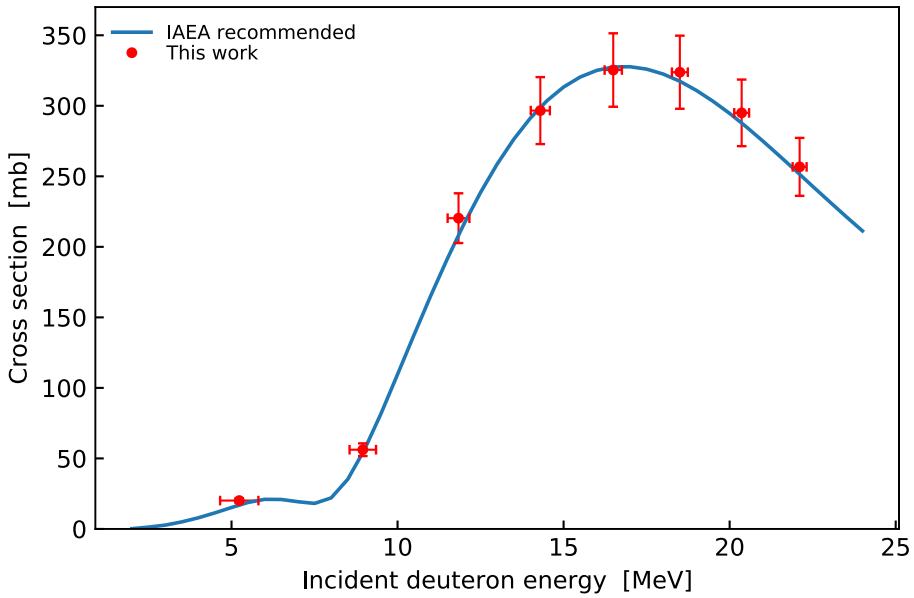

Fig. 1. Excitation function of the ^{nat}Ti(d,x)^{48}V monitor reaction compared with the IAEA recommended values [15].

3. Results and discussion

We confirmed formations of ^{89}Zr, ^{88}Zr, ^{90m}Y, ^{88}Y and ^{87m}Sr by the gamma-ray spectrometry. Their production cross sections including uncertainties are listed in Table 3 and displayed together with the previously published data [3–8,10,16–18]. The experiment published in 1973 [9] shows large discrepancies from the other data sets. Therefore, its results are omitted in the figures.

The total relative uncertainty (8-31.6%) of the cross sections was determined as the square root of the summed squares of the relative uncertainties of the parameters used in their calculation. Components of the total relative uncertainty cover beam intensity (5%), detector efficiency (5%), background subtraction (3%), target thickness (2%), target purity (1%) and statistical uncertainty (0.2-30.5%) of the net peak area of the particular gamma-ray.

Table 3. Production cross sections of each radionuclide obtained from this work.

	Cross section (mb)				
Energy (MeV)	^{89}Y(d,2n)^{89}Zr	^{89}Y(d,3n)^{88}Zr	^{89}Y(d,p)^{90m}Y	^{89}Y(d,x)^{88}Y	^{89}Y(d,x)^{87m}Sr
23.2±0.2	595±48	381±31	13.8±1.1	110±9	1.84±0.17
22.9±0.2	613±49	354±28	13.8±1.1	102±8	1.82±0.17
22.6±0.2	615±49	315±25	13.5±1.1	92.7±7.5	1.84±0.17
21.5±0.2	756±60	228±18	14.8±1.2	70.7±5.7	2.14±0.22
21.2±0.2	780±62	199±16	14.8±1.2	62.9±5.1	1.97±0.22
20.9±0.2	832±67	175±14	15.7±1.3	57.2±4.6	2.20±0.23
19.7±0.2	915±73	82.0±6.6	15.8±1.3	33.8±2.8	2.39±0.23
19.4±0.2	909±73	62.8±5.0	15.7±1.3	27.8±2.3	2.21±0.22
19.1±0.2	923±74	46.2±3.7	15.4±1.3	23.4±1.9	2.15±0.28
17.8±0.2	964±77	13.6±1.1	16.7±1.4	13.9±1.2	2.43±0.25
17.5±0.2	961±77	7.43±0.65	17.3±1.4	12.0±1.1	2.23±0.22
17.1±0.3	942±75	3.99±0.45	17.0±1.4	11.2±1.0	2.56±0.26
15.8±0.3	894±72		17.8±1.4	8.91±0.78	2.51±0.24
15.4±0.3	872±70		17.6±1.4	8.09±0.71	2.64±0.23
15.0±0.3	910±73		19.1±1.5	8.48±0.77	2.61±0.25
13.5±0.3	836±67		19.9±1.6	5.45±0.52	3.01±0.27
13.1±0.3	771±62		19.2±1.6	4.61±0.44	2.66±0.25
12.6±0.3	759±61		19.9±1.6	3.77±0.4	2.86±0.26
10.9±0.3	564±45		18.5±1.5	1.42±0.22	2.43±0.21
10.4±0.4	528±42		19.2±1.5	0.913±0.231	2.39±0.22
9.9±0.4	469±38		18.8±1.5	0.665±0.210	2.21±0.20
7.8±0.4	130±10		11.4±0.9		0.999±0.101
7.2±0.5	62.9±5.0		9.01±0.73		0.740±0.086
6.6±0.5	15.6±1.3		5.89±0.48		0.424±0.051
3.5±0.8			0.0872±0.0082		
2.5±1.0			0.00909±0.00193		

3.1 The ^{89}Y(d,2n)^{89}Zr reaction

The cross sections of the ^{89}Y(d,2n)^{89g}Zr reaction were derived using measurements of the 909.15-keV gamma line ($I_\gamma = 99.04\%$) emitted in the decay of ^{89g}Zr ($T_{1/2} = 78.41$ h). The meta-stable state of ^{89}Zr, ^{89m}Zr (IT: 93.77%, EC: 6.23%), has a half-life of 4 min and decays completely during a short cooling time of less than an hour. The cumulative cross sections including contributions from ^{89m}Zr were determined and are shown in Fig. 2 with the previous studies [3–8,10] and the TENDL-2017 values [19]. Our experimental data are consistent with the latest four works [3–6]. The TENDL-2017 values are larger than all experimental data in the energy region between 6 and 20 MeV.

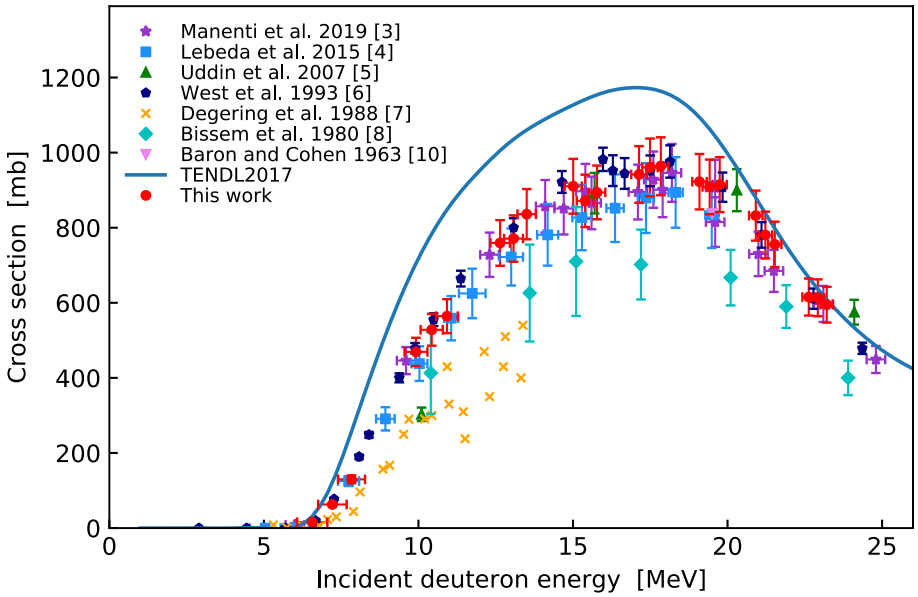

Fig. 2. Excitation function of the ^{89}Y(d,2n)^{89}Zr reaction compared with the previous experimental data [3–8,10] and the TENDL-2017 values [19].

3.2 The ^{89}Y(d,3n)^{88}Zr reaction

To estimate radionuclidic impurities isotopic with ^{89g}Zr the production cross sections of ^{88}Zr ($T_{1/2} = 83.4$ h) are necessary. The 392.87-keV gamma line ($I_\gamma = 97.29\%$) was measured to derive cross sections of the ^{89}Y(d,3n)^{88}Zr reaction. The cooling time from the end of the irradiation was about 2 weeks.

Figure 3 shows our result in comparison with the previous researches [3–6,8] and the TENDL-2017 values [19]. All the experimental datasets roughly agree with each other. The TENDL-2017 values are higher than the experimental data.

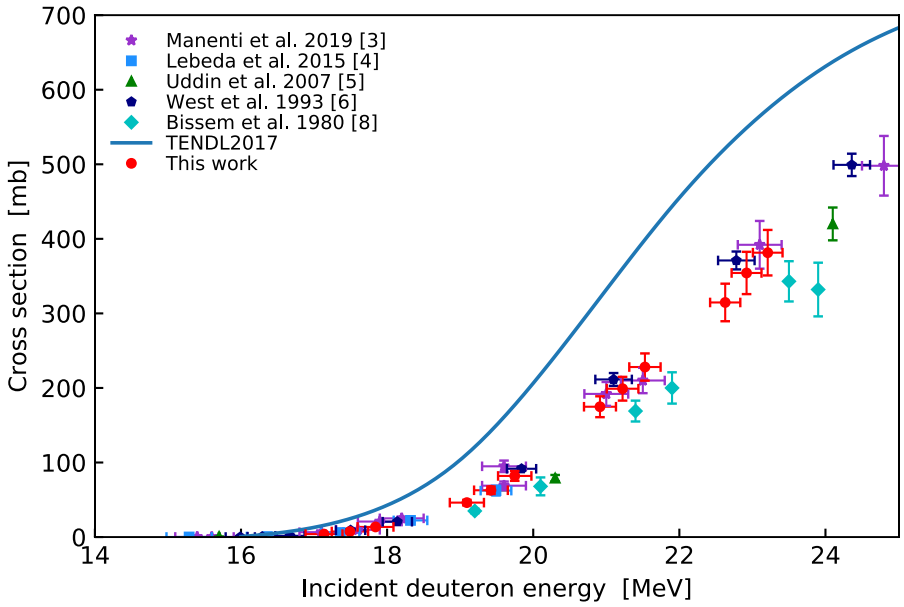

Fig. 3. Excitation function of the ^{89}Y(d,3n)^{88}Zr reaction compared with the previous experimental data [3–6,8] and the TENDL-2017 values [19].

3.3 The ^{89}Y(d,p)^{90m}Y reaction

Gamma-ray measurements at 202.53 keV ($I_\gamma = 97.3\%$) were performed to derive the excitation function of the ^{89}Y(d,p)^{90m}Y reaction. The cooling time was about 1-3 hours for the shorter-lived radionuclide ^{90m}Y ($T_{1/2} = 3.19$ h).

The derived excitation function is shown in Fig. 4 with the previous works [4,6,8,16–18] and the TENDL-2017 values [19]. Except for one dataset [17], the experimental data are quite consistent with each other within their uncertainties. On the other hand, the TENDL-2017 values are quite different from the experimental data.

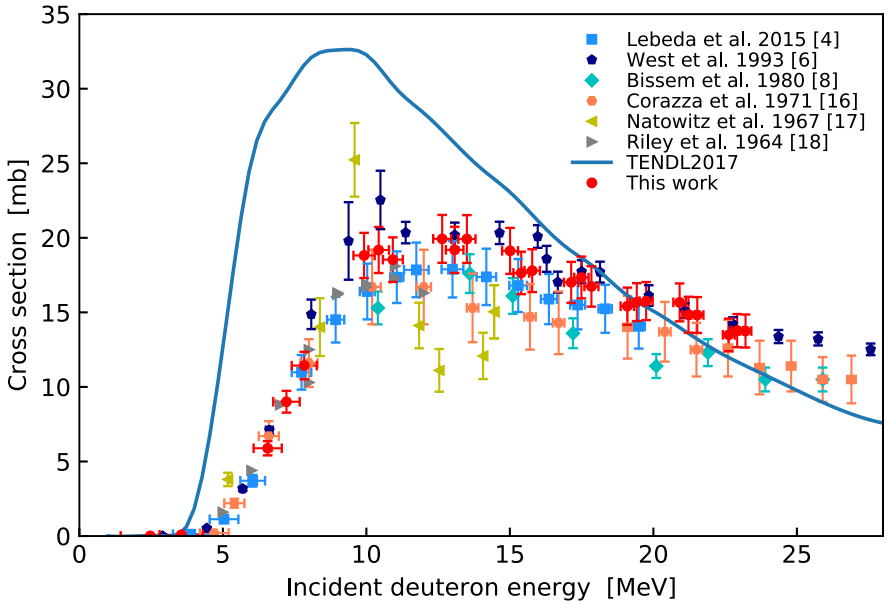

Fig. 4. Excitation function of the ^{89}Y(d,p)^{90m}Y reaction compared with the previous experimental data [4,6,8,16–18] and the TENDL-2017 values [19].

3.4 The ^{89}Y(d,x)^{88}Y reaction

The excitation function of the ^{89}Y(d,x)^{88}Y reaction was derived by measuring the gamma line at 898.042 keV (I_γ = 93.7%). The contribution of ^{88}Zr was calculated from the cross sections obtained in section 3.2 and subtracted from the measured counts of the gamma line. The independent cross sections to produce ^{88}Y ($T_{1/2}$ = 106.627 d) were obtained and are shown in Fig. 5 compared with previous works [3–6,8] and the TENDL-2017 values [19]. The previous studies show a good agreement with our results. The TENDL-2017 values are slightly higher than the experimental data above 19 MeV.

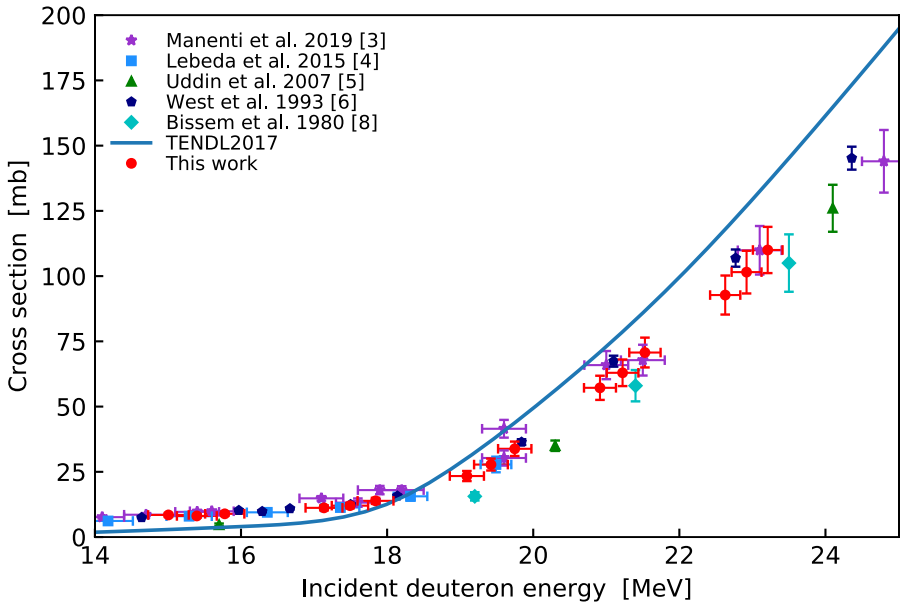

Fig. 5. Excitation function of the ^{89}Y(d,x)^{88}Y reaction compared with the previous experimental data [3–6,8] and the TENDL-2017 values [19].

3.5 The ^{89}Y(d,x)^{87m}Sr reaction

The cross sections of the ^{89}Y(d,x)^{87m}Sr reaction were determined based on measurements of the 388.531-keV gamma line ($I_\gamma = 82.19\%$). The measurements were performed after a cooling time of about 1-3 hours due to the short half-life of ^{87m}Sr ($T_{1/2} = 2.815$ h). The statistical component of the cross sections uncertainty (4.8-8.2%) is larger than in the case of the other reactions due to low counting statistics at this gamma line.

The result is shown in Fig. 6 in comparison with the earlier experimental data [4,6,8] and the TENDL-2017 values [19]. All the experimental data show their peaks at around 14 MeV. The TENDL-2017 values underestimate all the experimental data in the whole energy region.

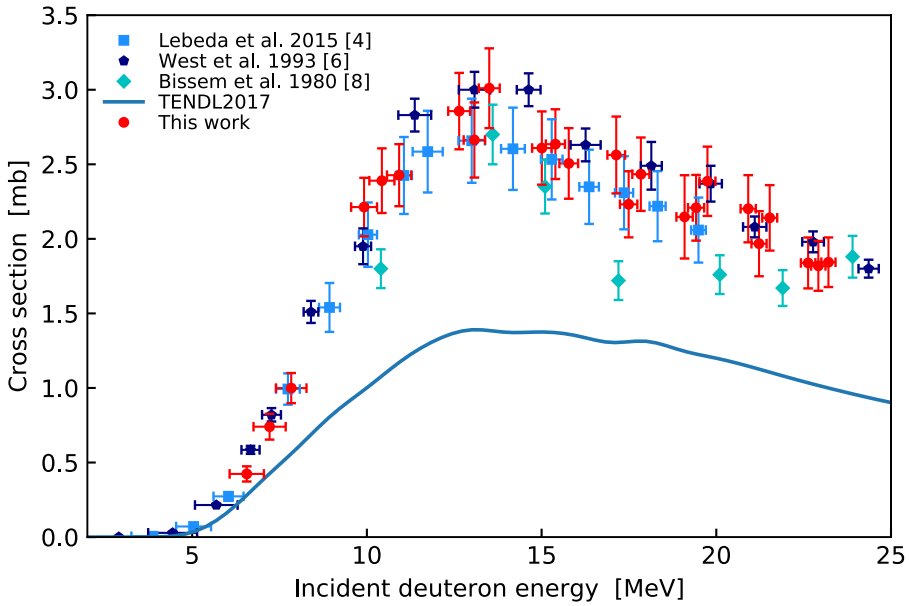

Fig. 6. Excitation function of the ^{89}Y(d,x)^{87m}Sr reaction compared with the previous experimental data [4,6,8] and the TENDL-2017 values [19].

3.6 Physical thick target yield of ^{89}Zr

We calculated physical thick target yields [20] of ^{89}Zr from the cross sections measured in this work and stopping powers calculated by the SRIM code [12]. The result is shown in Fig. 7 and compared with that of the ^{89}Y(p,n)^{89}Zr reaction [2].

In a low energy region, we can obtain more ^{89}Zr by using the ^{89}Y(p,n)^{89}Zr reaction than the ^{89}Y(d,2n)^{89}Zr reaction. However, above 21.2 MeV, the yield of the deuteron-induced reaction becomes larger than that of the proton-induced reaction. In addition, the ratio of an isotopic impurity ^{88}Zr to ^{89}Zr in the deuteron-induced reaction can be smaller than in the proton-induced one at energies above 16.2 MeV as discussed in the recent papers [3,4]. Therefore, the deuteron-induced reaction may be more favorable route than the proton-induced one.

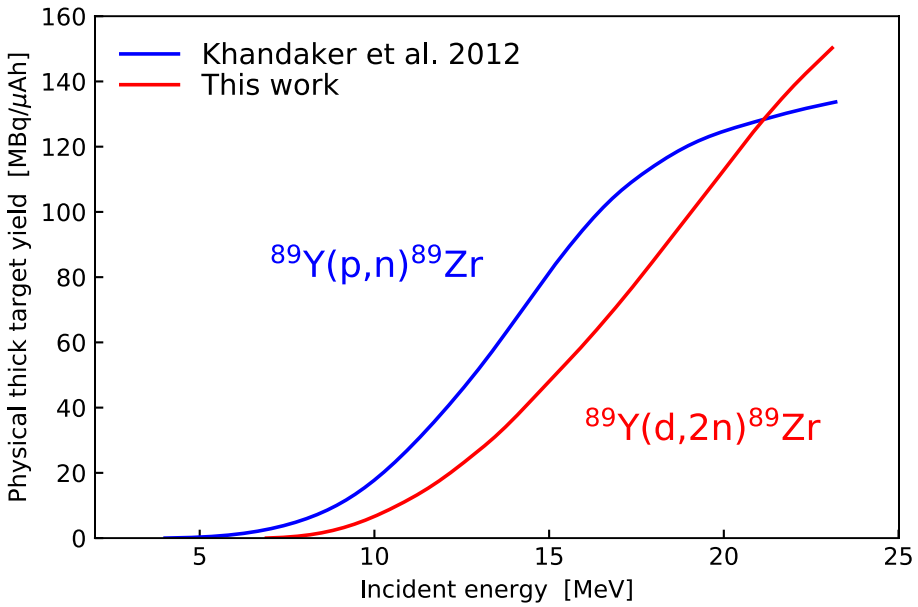

Fig. 7. Comparison of physical thick target yields of ^{89}Zr in the ^{89}Y(d,2n) and ^{89}Y(p,n) reactions.

4. Summary

Activation cross sections of the deuteron-induced reaction on ^{89}Y were measured up to 24 MeV at the RIKEN AVF cyclotron. We used the stacked-foil activation method and the gamma-ray spectrometry. The excitation functions for formation of the ^{89}Zr, ^{88}Zr, ^{90m}Y, ^{88}Y and ^{87m}Sr radionuclides were obtained and compared with the previous studies and the TENDL-2017 values. We calculated physical thick target yield of ^{89}Zr from the cross sections measured in this work and found that the deuteron-induced reaction on ^{89}Y provides higher yield of ^{89}Zr than the proton-induced reaction above 21.2 MeV particle energy. The obtained results are of interest for estimating optimal production route for ^{89}Zr, its radionuclidic purity and nuclear reaction model codes.

Declaration of Competing Interest

The authors have no conflicts of interest in this paper.

Acknowledgments

This work was carried out at RI Beam Factory operated by RIKEN Nishina Center and CNS, University of Tokyo, Japan. This work was supported by JSPS KAKENHI Grant No. 17K07004.

References

[1] M.A. Deri, B.M. Zeglis, L.C. Francesconi, J.S. Lewis, PET imaging with 89Zr: From radiochemistry to the clinic, Nucl. Med. Biol. (2013). https://doi.org/10.1016/j.nucmedbio.2012.08.004.

[2] M.U. Khandaker, K. Kim, M.W. Lee, K.S. Kim, G. Kim, N. Otuka, Investigations of 89Y(p,x) 86,88,89gZr, 86m+g,87g,87m,88gY, 85gSr, and 84gRb nuclear processes up to 42 MeV, Nucl. Instruments Methods Phys. Res. Sect. B Beam Interact. with Mater. Atoms. (2012). https://doi.org/10.1016/j.nimb.2011.11.009.

[3] S. Manenti, F. Haddad, F. Groppi, New excitation functions measurement of nuclear reactions induced by deuteron beams on yttrium with particular reference to the production of 89Zr, Nucl. Instruments Methods Phys. Res. Sect. B Beam Interact. with Mater. Atoms. 458 (2019) 57–60. https://doi.org/10.1016/j.nimb.2019.08.002.

[4] O. Lebeda, J. Štursa, J. Ráliš, Experimental cross-sections of deuteron-induced reaction on ^{89}Y up to 20 MeV; comparison of ^{nat}Ti(d,x)^{48}V and ^{27}Al(d,x)^{24}Na monitor reactions, Nucl. Instruments Methods Phys. Res. Sect. B. 360 (2015) 118–128. https://doi.org/10.1016/j.nimb.2015.08.036.

[5] M.S. Uddin, M. Baba, M. Hagiwara, F. Tárkányi, F. Ditrói, Experimental determination of deuteron-induced activation cross sections of yttrium, Radiochim. Acta. 95 (2007) 187–192. https://doi.org/10.1524/ract.2007.95.4.187.

[6] H.I. West Jr., R.G. Lanier, M.G. Mustafa, R.M. Nuckolls, R.J. Nagle, H. O'Brien, Some light-ion excitation-function measurements on titanium, yttrium, and europium, and associated results, Lawrence Livermore National Laboratory, Livermore, California, 1993.

[7] D. Degering, S. Unterricker, W. Stolz, Excitation function of the 89Y(d,2n)89Zr reaction, J. Radioanal. Nucl. Chem. Lett. 127 (1988) 7–11. https://doi.org/10.1007/BF02165500.

[8] H.H. Bissem, R. Georgi, W. Scobel, J. Ernst, M. Kaba, J.R. Rao, H. Strohe, Entrance and exit channel phenomena in d- and ^{3}He-induced preequilibrium decay, Phys. Rev. C. 22 (1980) 1468.

https://doi.org/10.1103/PhysRevC.22.1468.

[9] A.M. La Gamma, S.J. Nassiff, Excitation Functions for Deuteron-Induced Reactions on ^{89}Y, Radiochim. Acta. (1973) 161–162. https://doi.org/10.1524/ract.1973.19.4.161.

[10] N. Baron, B.L. Cohen, Activation cross-section survey of deuteron-induced reactions, Phys. Rev. 129 (1963) 2636–2642. https://doi.org/10.1103/PhysRev.129.2636.

[11] T. Watanabe, M. Fujimaki, N. Fukunishi, H. Imao, O. Kamigaito, M. Kase, M. Komiyama, N. Sakamoto, K. Suda, M. Wakasugi, K. Yamada, Beam energy and longitudinal beam profile measurement system at the RIBF, in: Proc. 5th Int. Part. Accel. Conf. (IPAC 2014), 2014: pp. 3566–3568.

[12] J.F. Ziegler, J.P. Biersack, M.D. Ziegler, SRIM: the Stopping and Range of Ions in Matter, (2008). http://www.srim.org.

[13] B. Pritychenko, A. Sonzogni, Q-value Calculator (QCalc), (2003). http://www.nndc.bnl.gov/qcalc/.

[14] National Nuclear Data Center, Nuclear structure and decay data on-line library, Nudat 2.7, (2017). http://www.nndc.bnl.gov/nudat2/.

[15] A. Hermanne, A. V. Ignatyuk, R. Capote, B. V. Carlson, J.W. Engle, M.A. Kellett, T. Kibédi, G. Kim, F.G. Kondev, M. Hussain, O. Lebeda, A. Luca, Y. Nagai, H. Naik, A.L. Nichols, F.M. Nortier, S. V. Suryanarayana, S. Takács, F.T. Tárkányi, M. Verpelli, Reference Cross Sections for Charged-particle Monitor Reactions, Nucl. Data Sheets. 148 (2018) 338–382. https://doi.org/10.1016/j.nds.2018.02.009.

[16] C. Corazza, S.J. Nassiff, Cross Sections and Isomer Ratios for the Isomeric Pair 90mY and 90gY in the 89Y (d,p) Reaction, Radiochim. Acta. (1971). https://doi.org/10.1524/ract.1971.15.1.7.

[17] J.B. Natowitz, R.L. Wolke, Isomeric cross sections and yield ratios of (d,p) reactions below 15 MeV, Phys. Rev. (1967). https://doi.org/10.1103/PhysRev.155.1352.

[18] C. Riley, B. Linder, Cross sections and isomer ratios for the isomeric pair Y^{90g} and Y^{90m} in the Rb^{87}(α,n) and Y^{89}(d,p) reactions, Phys. Rev. 134 (1964) B559.

[19] A.J. Koning, D. Rochman, J. Sublet, N. Dzysiuk, M. Fleming, S. van der Marck, TENDL: Complete Nuclear Data Library for Innovative Nuclear Science and Technology, Nucl. Data Sheets. 155 (2019) 1–55. https://doi.org/10.1016/j.nds.2019.01.002.

[20] N. Otuka, S. Takács, Definitions of radioisotope thick target yields, Radiochim. Acta. 103 (2015) 1–6. https://doi.org/10.1515/ract-2013-2234.